Journal of Engineering and Applied Sciences 14 (17): 6371-6384, 2019
ISSN: 1816-949X

Design and Implementation of a Teleoperation and Remote Monitoring System for a Prototype of Water Purification Powered by Photovoltaic Solar Energy

Javier Vargas, Wilder Herra and Fernando Riveros
Faculty of Basic Sciences and Engineering,
EYSI Research Group, Macrypt Research Group,
Universidad De Los Llanos (University of the Llanos), Villavicencio, Colombia

Abstract: This study describes the development of a tele-operation and remote monitoring system for a prototype of water purification based on photovoltaic solar energy. The implementation was carried out by integrating web service, artificial vision technologies and free software with the objective of taking a photographic capture of a multi-parameter Hi 9813-6n Hanna instruments device (responsible for measuring parameters related to water quality inside the water maker) and process the images to present data in alpha-numerical format in real time through a web application including also evidence of image processing, character recognition and the status of the multiparameter battery. The system performed the image processing and subsequent character recognition by implementing the OpenCV library under the Python language and allowed real-time access to information to multiple users from any point connected to the internet through a Node.js web application displayed on the Heroku infrastructure, additionally, video transmission was presented in the web application in order to know the state of the system and analyze its behavior in a more comprehensive manner.

Key words: Teleoperation, remote monitoring, internet at all, virtual instrumentation, digital image processing, web applications, cloud computing

INTRODUCTION

The geographical barriers that are established between the facilities of plants or production systems and the operators there of generate economic costs represented in the transportation of trained personnel to carry out periodic maintenance as well as a wear on the employees of said systems due to the complexity for perform monitoring and control activities, in addition, the difficulty for real-time access to sensor information is often causing some system failures which increases the economic costs in terms of repair and commissioning.

In the era of Internet of Things (IoT), remote access to any type of a system is becoming an essential part of its infrastructure. However, remote access under IoT conditions is usually understood as active or passive with some intelligence in the system or in the client software. Gaspar and Andoga (2018) active access represents a possibility of interactions with the system (teleoperation) while passive access presents only remote monitoring (Kress *et al*., 2001).

The development of remote access systems within industrial or productive processes brings with it some positive changes such as better response time to emergency situations, greater comfort for operation and greater efficiency related to the calibration of systems by individual operators this represents a advantage over competitors that do not implement remote monitoring technologies and therefore an increase in the economic profits of companies (Hall and Harrington, 2005). Besides, these systems can also provide tools to carry out distance education where students from a virtual environment can relate to a real industrial environment, achieving a training of the basic principles of operation, reducing the level of abstraction that inherently exists in the teaching subjects that require laboratory practices (Martin *et al*., 2003).

OCR is the electronic conversion of images into machine-coded text. Provides alpha numeric characters recognition of printed or hand written characters (Sonth and Kallimani, 2017).

To carry out the OCR in this research was used OpenCV, a cross-platform computer vision library with an

Corresponding Author: Javier Vargas, Researchers Faculty of Basic Sciences and Engineering, EYSI Research Group, Macrypt Research Group, Universidad De Los Llanos (University of the Plains), Villavicencio, Colombia

open source that started as a research project in Intel in 1998 and has been available, since, 2000. OpenCV aims to provide the tools necessary to develop projects related to artificial vision can be implemented in a large number of languages such as C++, C, Python, JavaScript and Android, contains a mixture of low-level image processing with functions and high level algorithms (Xu *et al*., 2017).

Cloud computing or cloud computing allows offering multiple services through a single platform (Internet), the main philosophy of this new paradigm of technology is to provide solutions of all kinds as a service, so that, users can access resources available in the internet cloud without knowledge of the management of the systems they use. The cloud computing servers distribute data servers around the world in order to reduce connection times oriented to access and real-time query of data. There are three major sets of services that can be established in cloud computing, Software as a Service (SaaS), Platform as a Service (PaaS) and Infrastructure as a Service (IaaS).

PubNub is an Infrastructure as a Service (IaaS) that offers the possibility of communicating messages in JSON format in real time under the publish/sucribe technique. PubNub offers a set of SDKs that allow using the infrastructure with different programming languages, (Sangjun *et al*., 2017) the operation of PubNub can be presented in a fairly simple way, first, the platform establishes a publication and subscription key for the writing and reading of a channel then a channel is enabled in which it is possible to publish messages from any device that have the publication key these messages are read in real time in <2 sec by all devices connected to that channel and that have the subscription key.

The implementation of a system that uses artificial vision for the segmentation and Character Recognition (OCR) of the data coming from a multi-parameter meter of temperature, pH, EC and TDS, later sends the readings to a web application deployed on a platform is presented cloud to allow access to information to multiple users from any point connected to the internet.

MATERIALS AND METHODS

Hardware: To know the state of the water that is processed in the potabilizer an HI 9813-6 was used, a portable multiparameter device developed for the measurement of temperature, pH, EC and TDS in liquids which has applications in agriculture, hydroponics, greenhouses, farms and nurseries, among many others. The image capture of the device was achieved using a generic webcam with an approximate value of 6 USD which allowed to reduce costs in the acquisition of a high quality camera (Fig. 1).

Fig. 1: HI 9813-6 Hanna instruments

To guarantee the uniform capture of the images and thus, achieve a more agile processing of them, a support was built where the camera was at the same distance from the multiparameter and focusing the same point in a constant manner for the construction of the support some location tests, taking measurements and their respective digital modeling (Fig. 2).

With the digital model of the support, the structure is intended to be printed in 3D but prior to this a wooden prototype is constructed in order to detect possible design flaws (Fig. 3 and 4).

El soporte en madera permitio realizar las primeras pruebas de software operation for the whole system, it is

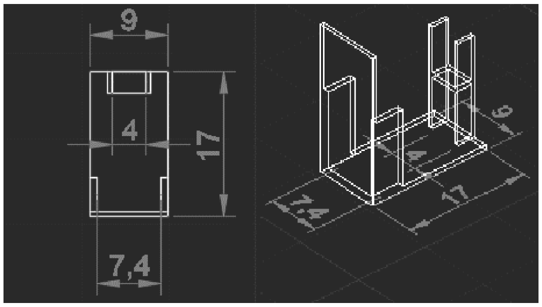

Fig. 2: 3D modeling of the support

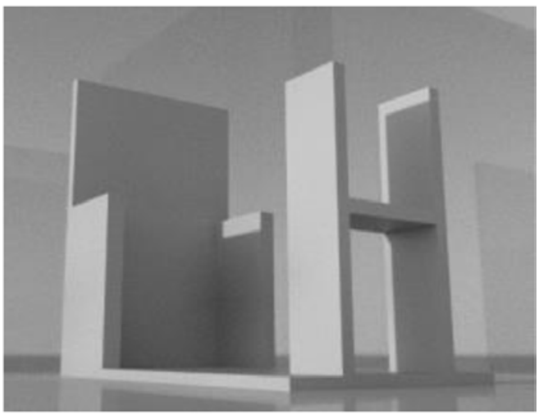

Fig. 3: Digital model of the prototype of support

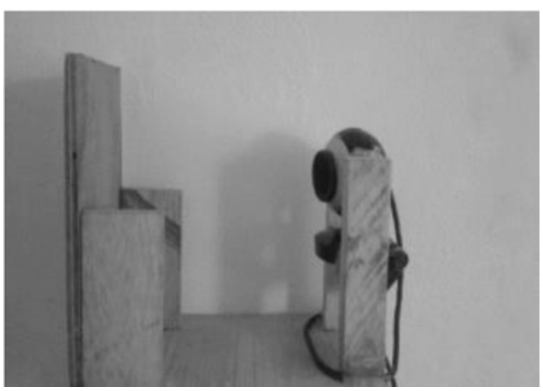

Fig. 4: Prototype in wood of the support with installed camera

established that the OCR is working and that the data to the web application is being received in real time if without any type of error (Fig. 5).

After testing the support, it is concluded that the location of the camera is correct and therefore, the measures established in the digital design are satisfactory but when generating the file for 3D printing it is

Fig. 5: System working with wooden support prototype

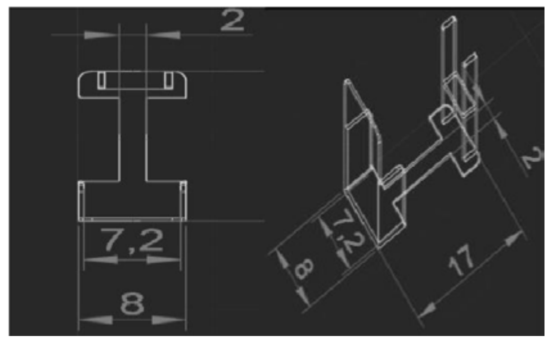

Fig. 6: Digital model of optimized support

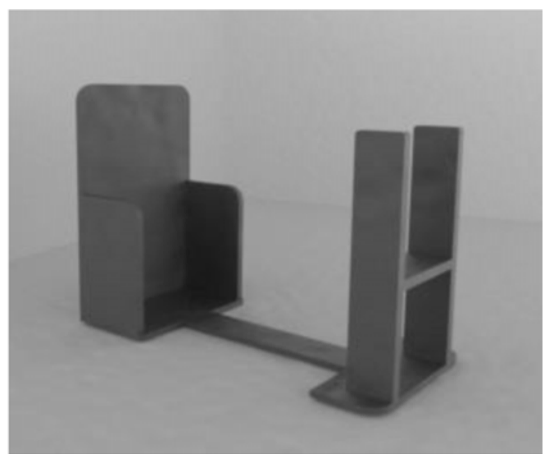

Fig. 7: Digital model of optimized support for 3D printing

discovered that a large amount of material is wasted in parts that are not vital for the support, so, we proceed to the optimization of the design.

Figure 6 be presented the measurements and digital design for optimized support, it can be noticed that it has a design that demands less printing material, since, it suppresses unnecessary parts besides having the thickness more reduced than the original design these modifications translate into less print material and a shorter print time (Fig. 7).

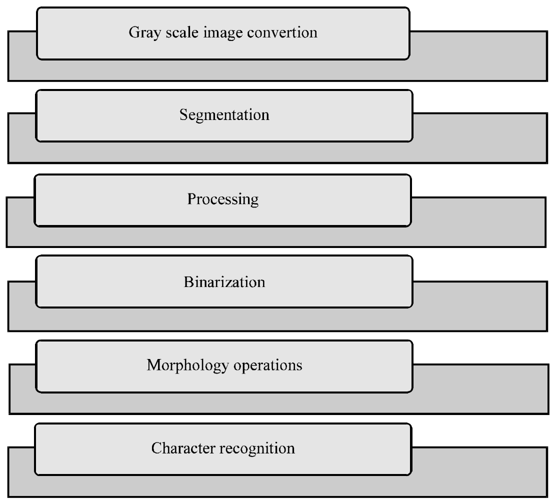

Fig. 8: Phases for the implementation of OCR

Artificial vision for segmentation and Character Recognition (OCR): The implementation of the processing system, segmentation and Character Recognition (OCR) was based on Python (a free-object oriented multi-paradigm programming language) and the OpenCV library. The phases for this development are presented (Fig. 8):

Grayscale image conversion: The images contain three layers (RGB) encapsulated which are responsible for representing the color, the conversion to gray scale allows these three layers to be contained in a single one that will contain the properties of the original image as well as facilitate digital processing.

Figure 9 shows the gray-scale color conversion of the image captured by the camera from the support, it can be seen that the color property is lost, besides mathematically the image can be seen as a single matrix unlike the image a color that is represented by three matrices.

Fig. 9a, b): Conversion of color to gray scale

Segmentation: Eliminating all parts of the image that do not provide information relevant to the recognition process and that cause a load to the processing system is called segmentation, it is a process that is established whenever you want to develop artificial vision applications and that allows to reduce noise levels and more efficient filtering or pre-processing in terms of speed because the image is smaller.

Figure 10 shows the segmented image with the information that is desired for the future filtering and recognition process in this process the original image is recovered only to the space that contains the screen of the meter eliminating the rest of unnecessary information.

Fig. 10: Segmented image

Processing: In image processing, a Gaussian filter is used to "Blur" the image and obtain a smoothing of the image, the Gaussian blur filter is used to eliminate noise and as a pre-processing step to improve the structure of the image. image.

Mathematically, applying a Gaussian filter to an image is similar to the convolution of the image to be filtered with the Gaussian function (Singhal *et al*., 2017). In one dimension the Gaussian function has the form of Eq. 1 by transforming this equation for two dimensions we obtain the Eq. 2:

$$G(x) = \frac{1}{2\pi\sigma^2} e^{\frac{x^2}{2\sigma^2}} \quad (1)$$

$$G(x, y) = \frac{1}{2\pi\sigma^2} e^{\frac{x^2+y^2}{2\sigma^2}} \quad (2)$$

The histogram is a bar chart whose abscissas represent the gray levels of an image and the ordinates, the relative frequencies of the different levels of gray that is the number of points associated with each level of gray, divided by the amount total points of the image Eq. 3:

$$Pk = \frac{Nk}{N} \quad (3)$$

Where:
Nk = Pixels quantity K
N = Total quantity of pixels

Equation 4 defines a point operation that at each pixel of gray level k, transforms it into a gray level pixel F (k), achieving an extension of the dynamic range of the given image:

$$F(k) = 255 \sum_{i=0}^{k} Pi \qquad \text{To } 0 \leq k \leq 255 \quad (4)$$

During the process of acquiring the image, noises appear in the image caused by abrupt lighting changes and in addition to the noise, added by the camera due to its quality. To solve these imperfections, a combination of Gaussian smoothing filters and histogram equalization techniques was applied which allowed to reduce the impacts of ambient light during the image acquisition process to obtain a cleaner image prior to the binarization and recognition.

To solve these imperfections, a combination of Gaussian smoothing filters and histogram equalization techniques was applied which allowed to reduce the impacts of ambient light during the image acquisition process to obtain a cleaner image prior to the binarization and recognition. Figure 11 shows the evolution of the image due to the processing performed, it can be noted that the changes in ambient lighting for photo C are not so, noticeable and that a much more regular and noise-free image is obtained.

Binarization: Image binarization is a digital image processing technique that converts an original image into a new digital image formed only by values of 0 or 255, under the operating principles of the adaptive threshold a different threshold is set for each pixel based on the value of neighboring pixels.

The Otsu method was presented by Nobuyuki Otsu. This thresholding method is an automatic binarization level decision based on the histogram (Razali *et al*., 2014), the Otsu algorithm calculates the threshold value, so that, the dispersion within each segment is as small as possible but at the same time the dispersion is as high as possible between different segments (Vertan *et al*., 2017). For this, the quotient between both variances is calculated and a

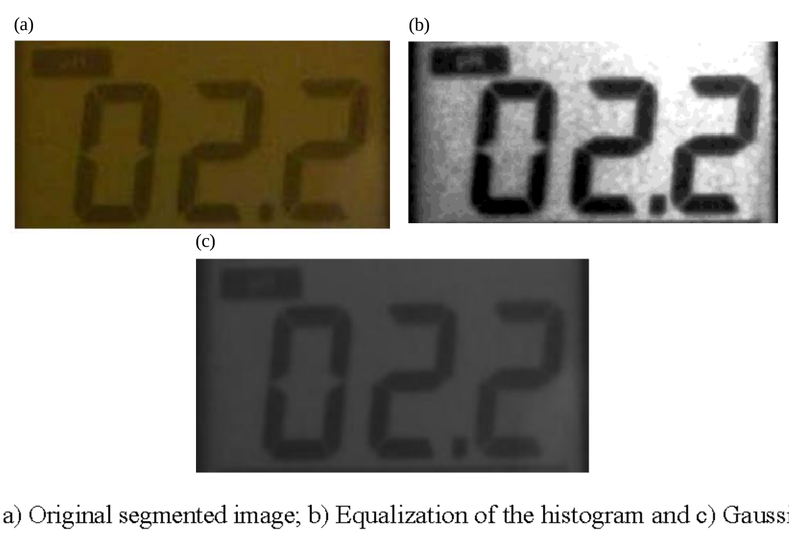

Fig. 11: Image filtering: a) Original segmented image; b) Equalization of the histogram and c) Gaussian smoothing filters

(a)

(b)

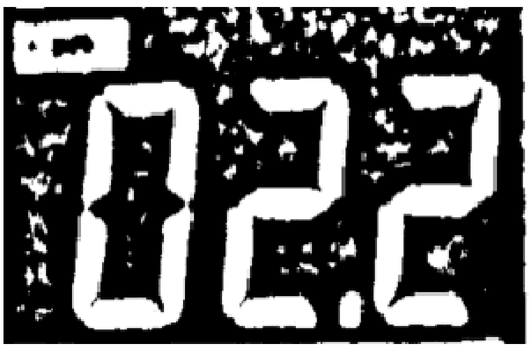

Fig. 12: a, b) Image binarization with thresholding by Otsu algorithm

(a)

(b)

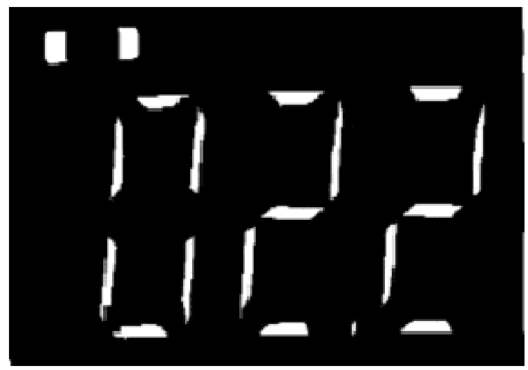

Fig. 13: a, b) Image morphology

threshold value is sought for which this quotient is maximum. The values of the image that are greater than the threshold take a value 255 (white), the rest of the pixels take the value 0 (black) (Fig. 12).

Morphology: Morphological operations simplify images and preserve the main shape characteristics of objects. Mathematical morphology is based on set theory operations. In the case of binary images, the treated sets are subsets of Z^2 and in the case of the grayscale images they are sets of points with coordinates in Z^2.

The morphological processing of an image allows, eliminate edges, fill regions, lose weight, swell, among other benefits to perform this process must necessarily convert to a grayscale image and then apply the function of binarization (Herrera *et al*., 2017).

Dilation and erosion are the two main morphological operations on binarized images for the development of this research we only used cascade erosion with 4 iterations for processing the captured images. The image erosion is defining in Eq. 5:

$$A\theta B = \{X|BxCA\} \quad (5)$$

The process of morphological erosion “Fig. 13” is applied with the objective of eliminating the small regions that are established as noise within the region that is considered useful and that could possibly generate disadvantages in the recognition. After obtaining the binarized and filtered image, we proceed to the recognition of the characters inside the multiparameter device screen.

First, it is established that the numbers inside the multiparameter screen have a 7-segment format that is these numbers are formed by the combination of some small individual segments. Taking into account the above, a new segmentation of the image is made where each of the numbers are individually isolated to later evaluate the segments that compose them and be able to give recognition to thenumber that is being visualized.

After obtaining the numbers individually, a new segmentation is made where each of the segments of the number is evaluated as indicated in Fig. 14 in order to establish which of those segments are active and thus, make the identification of the number.

In Mathematics, a matrix norm is an extension of the natural notion of vector norm to matrices. The calculation of the matrix standard of each of the segments that make

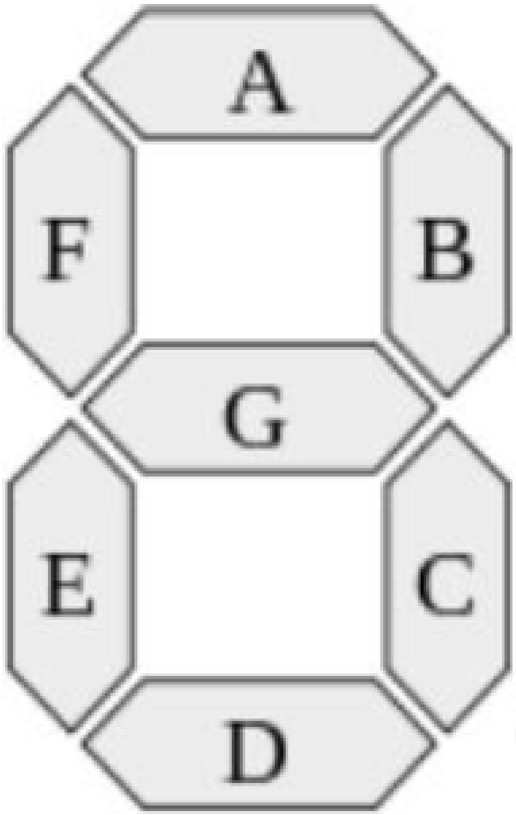

Fig. 14: Segments that make up a number within seven segments display

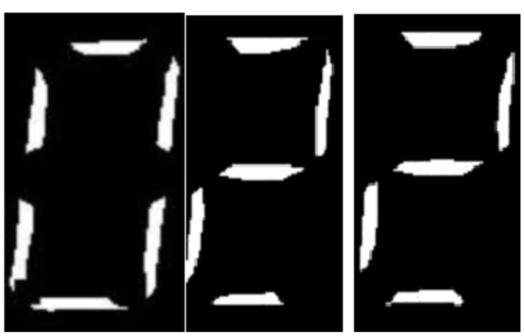

Fig. 15: Individual segmentation of the numbers on the screen

up the number on the screen was used to identify which of the segments are active and which of these are inactive (Fig. 15).

Next, each of the segments that make up the number 0 is shown. It can be noted that all the segments are active except for G which allows us to establish that in fact the number in question is zero (Fig. 16 and 17).

In addition to the recognition of the numbers presented on the screen, a reading of the battery status is also made in order to present the load level of the device

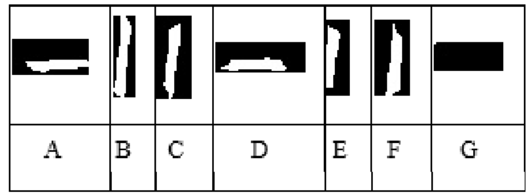

Fig. 16: Decomposed segments for the No. "0"

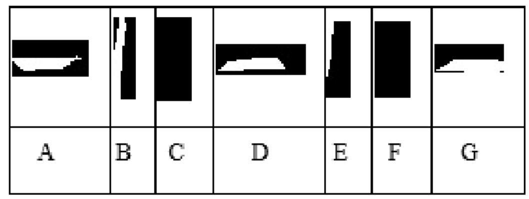

Fig. 17: Decomposed segments for No. 2

Fig. 18: Battery indicator in multiparameter device

in the web application. To achieve this, the norm of the image that contains the state of the battery in the device is evaluated (Fig. 18).

Data transmision: For the management of the data, the PubNub platform with the Python SDK was used to transmit the data resulting from the recognition of the images in real time (Fig. 19-21).

The data is received and presented through a WEB application based on Node.Js deployed in Heroku an infrastructure as a service that allows the publication of applications on a public domain.

Figure 22 presents the main panel of the application where you have the information of the data that is being read by the multiparameter device, in addition, to the images that evidence the process of artificial vision. Additionally, the literal "D" indicates some options to which the user can access to visualize the transmission of video in real time of the potabilizer, vary the voltage of the electrocoagulation stage or access the database to generate data reports.

```
from pubnub.enums import PNStatusCategory
from pubnub.pnconfiguration import PNConfiguration
from pubnub.pubnub import PubNub, SubscribeListener
```

Fig. 19: Libraries required for the use of PubNub SDK

```
pnconfig = PNConfiguration()

pnconfig.publish_key = 'pub-c-6e938ef8-f0e6-4215-a092-824794c101e3'
pnconfig.subscribe_key = 'sub-c-53cabfec-3dd7-11e7-82b8-0619f8945a4f'

pubnub = PubNub(pnconfig)
```

Fig. 20: Publication and subscription credentials

```
my_listener = SubscribeListener()
pubnub.add_listener(my_listener)
pubnub.subscribe().channels('canal1').execute()
my_listener.wait_for_connect()
```

Fig. 21: Subscription to 'channel1' of PubNub

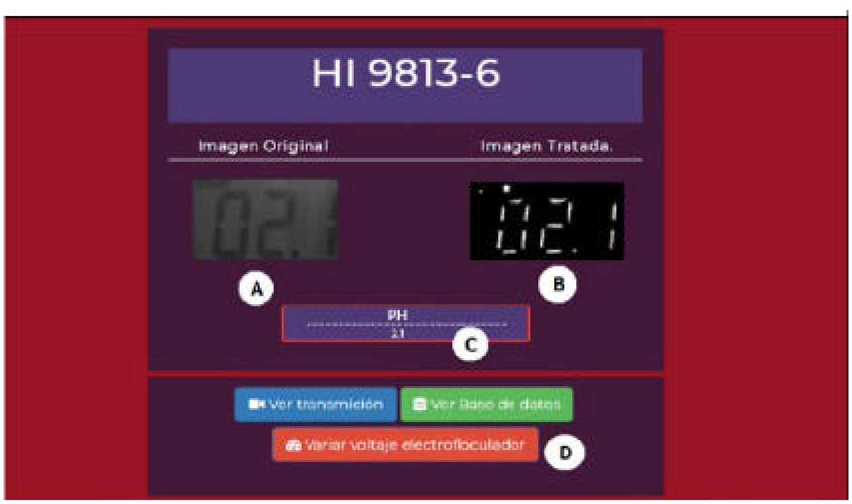

Fig. 22: Main panel of the web application: a) Original captured image of the multiparameter device; b) Processed image; c) Data in alpha-numeric of the measurement and d) Options for remote monitoring control

```
firebase=require("firebase")

var config = {
    apiKey: "AIzaSyD2DWr66AStgJtOKJGppe_ko7bDPkLDbk8",
    authDomain: "epiunillanos.firebaseapp.com",
    databaseURL: "https://epiunillanos.firebaseio.com",
    projectId: "epiunillanos",
    storageBucket: "epiunillanos.appspot.com",
    messagingSenderId: "994462945447"
  };

firebase.initializeApp(config);
database=firebase.database();
```

Fig. 23: Configuration of credentials and connection with database

```
app.get('/datos',(req,res)=>{
        console.log("datos");
        database.ref("/datos").push(req.body)
        res.status(200).end()
})
```

Fig. 24: Sending information packet to the "data" table

Database and report: A connection was implemented with a database hosted in the firebase cloud in order to create tables where the information captured by the multiparameter will be housed, in addition to the exact date and time of the capture.

Figure 23 shows the piece of code (JavaScript) that allows the connection to the database, it can be seen that it is necessary to have connection credentials that enable the application to host information within the database (Fig. 24).

Figure 25 shows the piece of code that carries out the publication of the information in the database, the process is simple, the information captured from the web application is received through a "GET" application and with the method "push" the file is sent in JSON format to a table called "data".

Figure 26 shows an example of an information package hosted in the non-relational database which contains among other information on the date of capture of the sample and the type and value of the captured data. With the information stored in the database, the user has the possibility of generating a report in PDF format that allows him to establish an analysis of the information collected.

Figure 26 shows the information search form within the application this form includes three search criteria, the day of measurement, the time of measurement and the type of data, when the user establishes the search criteria and press the "consult" button, a table with the information is displayed as well as a button that allows you to generate a downloadable PDF report as shown in Fig. 27 and 28.

Teleoperation: Electrocoagulation is one of the stages within the purification system responsible for water filtration through electrodes powered by DC current, Fig. 29 presents the electrocoagulation system with the circuit used for feeding it, the teleoperation system implemented for this project the objective was remote control of the feeding for the electro-coagulator.

To carry out the voltage control, the circuit presented in Fig. 30 was designed. This circuit has a

Fig. 25: Information package hosted in the database

Fig. 26: Form for data search

Fig. 27: Result of query to database

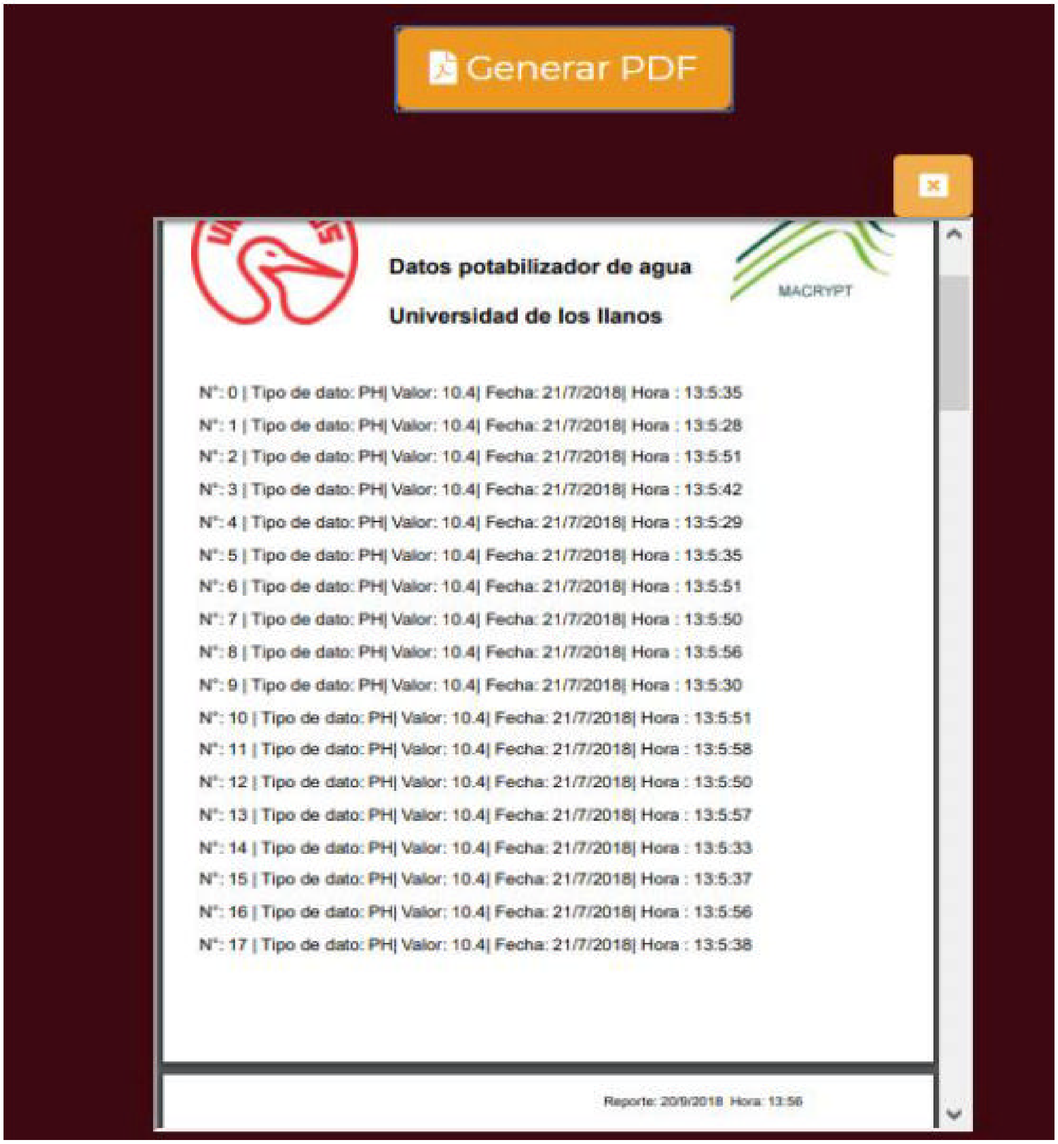

Fig. 28: Downloadable PDF report

rectification stage that allows the circuit to be connected to an AC input, a control stage where the DC output voltage is reclosed by a PWM signal from a microcontroller.

The PWM control signal was generated using an Arduino-type microcontroller system which varied the pulse width of the signal generated as a function of values received through the serial port these values were sent through a Python script that receives values from the web application and send them through the serial port. Using the bar shown in Fig. 31 it was possible to vary the voltage with which the electro-coagulator is fed in real time from the application.

Fig. 29: Electrocoagulation stage

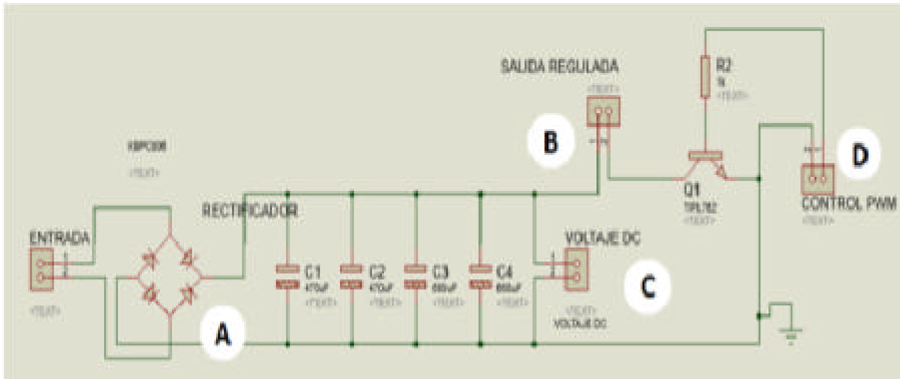

Fig. 30: Circuit for teleoperation; a) Rectification; b) DC regulated output; c) DC output without regulation and d) Control signal input

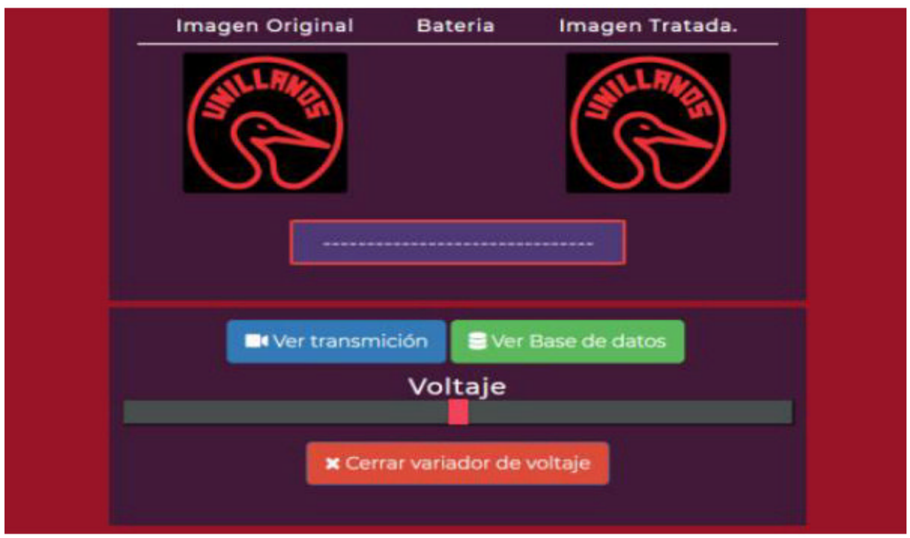

Fig. 31: Bar for voltage control in web application

RESULTS AND DISCUSSION

The remote monitoring system based on digital image processing was evaluated by sampling measurements in order to establish their precision and accuracy. For the evaluation of the device a sample of water mixed with sodium bicarbonate was used where the results for thirty samples of each type of data are presented Table 1.

Taking into account that the accuracy is defined as the degree of agreement between the result and a reference value and that the accuracy on the other hand is defined as the measure of the dispersion of a set of several measurements. The calculation of the accuracy and precision was based on the following equations accuracy:

$$\bar{x} = \frac{1}{n}\sum_{i=1}^{n} x_i \tag{6}$$

Precision:

$$\sigma = \sqrt{\frac{\sum_{i=1}^{n}\left(x_i-\bar{x}\right)^2}{n-1}} \tag{7}$$

According to Table 1, it can be established that the artificial vision system has a precision and accuracy of 100% in the sampling relative to the pH, conductivity (mS/cm) and temperature (°C) but in the sampling of the Particles Per Million (PPM), the system presents some erroneous results where there is evidence of a failure in the reading of the last digit. Finally, applying Eq. 6 and 7 on the data set, we obtain that the system has a precision of 98.5% and an accuracy of 99.38%.

Table 1: Data sampling

Valor real		Valor real		Valor real		Valor real	
pH (#)	0.92 (Valor)	C° (#)	27.9 (Valor)	mS/cm (#)	0.83 (Valor)	PPM (#)	591 (Valor)
1	0.92	1	27.9	1	0.83	1	597
2	0.92	2	27.9	2	0.83	2	591
3	0.92	3	27.9	3	0.83	3	597
4	0.92	4	27.9	4	0.83	4	597
5	0.92	5	27.9	5	0.83	5	591
6	0.92	6	27.9	6	0.83	6	597
7	0.92	7	27.9	7	0.83	7	597
8	0.92	8	27.9	8	0.83	8	597
9	0.92	9	27.9	9	0.83	9	591
10	0.92	10	27.9	10	0.83	10	591
11	0.92	11	27.9	11	0.83	11	597
12	0.92	12	27.9	12	0.83	12	591
13	0.92	13	27.9	13	0.83	13	597
14	0.92	14	27.9	14	0.83	14	597
15	0.92	15	27.9	15	0.83	15	597
16	0.92	16	27.9	16	0.83	16	591
17	0.92	17	27.9	17	0.83	17	597
18	0.92	18	27.9	18	0.83	18	591
19	0.92	19	27.9	19	0.83	19	597
20	0.92	20	27.9	20	0.83	20	597
21	0.92	21	27.9	21	0.83	21	597
22	0.92	22	27.9	22	0.83	22	591
23	0.92	23	27.9	23	0.83	23	597
24	0.92	24	27.9	24	0.83	24	591
25	0.92	25	27.9	25	0.83	25	597
26	0.92	26	27.9	26	0.83	26	591
27	0.92	27	27.9	27	0.83	27	591
28	0.92	28	27.9	28	0.83	28	597
29	0.92	29	27.9	29	0.83	29	597
30	0.92	30	27.9	30	0.83	30	597

CONCLUSION

The emergence of free technologies such as (Node.js, Python) that allows the free creation of software, in addition to infrastructure and cloud platforms (Heroku, PubNub) that deliver free dominoes for data transmission in real time, make the implementation of remote access systems can be inexpensive, thus, presenting a very positive scenario in the cost-benefit relationship.

The tools provided by the OpenCV library to implement digital image processing together with the advantages of the Python language in terms of writing and interpretation, allow for an agile development of the image processing and character recognition system with a fairly short, scalable source code. readable.

PubNub as an infrastructure allows it to send messages in real time with an average delivery time of 0.25 sec which made it possible for the remote monitoring and teleoperation system to deliver the real-time information of the multi parametric device measurements through the platform web deployed in the cloud, in addition to presenting the state of the battery and images that evidence the processing of images.

The process of image processing and character recognition presented a promised duration of 50 msec which guaranteed a sampling frequency (frame rate) around 20 Hz which translates into images and data being processed in real time and said processing it is transparent to the user.

The implementation of the system described in this study provides the basis for further developments aimed at distance education such as the construction of remote laboratories that contribute to the training of students in topics such as: process control, industrial automation and other courses with interactive methodologies that include laboratory practices.

REFERENCES

Gaspar, V. and R. Andoga, 2018. Proposal of an architecture for remote monitoring of systems using mobile and smart devices. Proceedings of the 2018 IEEE 16th World Symposium on Applied Machine Intelligence and Informatics (SAMI), February 7-10, 2018, IEEE, Kosice, Slovakia, ISBN:978-1-5386-4773-8, pp: 000179-000182.

Hall, J.L. and W.C. Harrington, 2005. Operate a wastewater treatment plant from the palm of your hand. Proc. Water Environ. Fed., 2005: 1603-1611.

Herrera, W.D., O.L. Leon, W.C. Londono and J.A. Vargas, 2017. Implementation of a control and biometric safety of the vascular network of the dorsal side of the hand through digital processing of images. Proceedings of the 2017 IEEE 3rd Colombian Conference on Automatic Control (CCAC), October 18-20, 2017, IEEE, Cartagena, Colombia, ISBN:978-1-5386-0399-4, pp: 1-6.

Kress, R.L., W.R. Hamel, P. Murray and K. Bills, 2001. Control strategies for teleoperated Internet assembly. IEEE. ASME. Trans. Mechatron., 6: 410-416.

Martin, S.C.S., V.F. Torres, R.S. Barrientos and M.D. Sandoval, 2003. [Monitoring and temperature control of a water tank between Chile and Spain using high speed networks (In Spanish)]. Faculty Eng. Mag. Chile., 11: 41-46.

Razali, M.R.M., N.S. Ahmad, Z.M. Zaki and W. Ismail, 2014. Region of adaptive threshold segmentation between mean, median and otsu threshold for dental age assessment. Proceedings of the 2014 International Conference on Computer, Communications and Control Technology (I4CT), September 2-4, 2014, IEEE, Langkawi, Malaysia, ISBN:978-1-4799-4555-9, pp: 353-356.

Sangjun, T., S. Aierpaiboon and C. Pintavirooj, 2017. New observing robot for elder. Proceedings of the 2017 10th International Conference on Biomedical Engineering (BMEiCON), August 31-Sept 2, 2017, IEEE, Hokkaido, Japan, ISBN:978-1-5386-0883-8, pp: 1-4.

Singhal, P., A. Verma and A. Garg, 2017. A study in finding effectiveness of Gaussian blur filter over bilateral filter in natural scenes for graph based image segmentation. Proceedings of the 2017 4th International Conference on Advanced Computing and Communication Systems (ICACCS), January 6-7, 2017, IEEE, Coimbatore, India, ISBN:978-1-5090-4560-0, pp: 1-6.

Sonth, S. and J.S. Kallimani, 2017. OCR based facilitator for the visually challenged. Proceedings of the 2017 International Conference on Electrical, Electronics, Communication, Computer and Optimization Techniques (ICEECCOT), December 15-16, 2017, IEEE, Mysuru, India, ISBN:978-1-5386-1205-7, pp: 1-7.

Vertan, C., C. Florea, L. Florea and M.S. Badea, 2017. Reusing the Otsu threshold beyond segmentation. Proceedings of the 2017 International Symposium on Signals, Circuits and Systems (ISSCS), July 13-14, 2017, IEEE, Iasi, Romania, ISBN:978-1-5386-0675-9, pp: 1-4.

Xu, Z., X. Baojie and W. Guoxin, 2017. Canny edge detection based on Open CV. Proceedings of the 2017 13th IEEE International Conference on Electronic Measurement and Instruments (ICEMI), October 20-22, 2017, IEEE Yangzhou, China, ISBN:978-1-5090-5036-9, pp: 2-5.